Mathematical Biology and Bioinformatics
2023. V. 18. № S. P. t38–t53. doi: 10.17537/2023.18.t38

Ttranslation of the original article
Trusov P.V. et al. Mathematical Biology and Bioinformatics. 2016;11(1):64–80.
doi: 10.17537/2016.11.64

========== **TRANSLATIONS OF PUBLISHED ARTICLES** ==========

Modeling of Human Breath: Conceptual and Mathematical Statements

Trusov P.V.[1,2], Zaitseva N.V.[1], Tsinker M.Yu.[*1,2]

[1]*Federal Scientific Center for Medical and Preventive Health Risk Management Technologies, Perm, Russia*
[2]*Perm National Research Polytechnic University, Perm, Russia*

Abstract. The article is devoted to the main aspects of the development of a mathematical model of the human respiratory system taking into account the effects of environmental factors. The proposed model is a submodel of "meso-level" multilayered mathematical model of the evolution of functional disorders of the human body. The conceptual and mathematical formulations of the problem are discussed. The breathing is considered as a set of synchronized processes of gas dynamics, deformation of the porous medium and diffusion. The results of the calculation of the air flow characteristics during quiet breathing and forced breath in the first four generations of large airways were obtained by using software ANSYS Fluent. Further development of the model involves the joint problem solving of changes in lung configuration and in gasdynamic processes in the human airway.

Key words: *mathematical simulation, respiratory system, functional disorders.*

1. INTRODUCTION

In their lifetime, people constantly interact with the environment. They get all the vital substances from it and simultaneously are exposed to harmful physical, chemical, biological and socioeconomic factors. Human health is analyzed by using laboratory and instrumental methods (x-ray examinations, endoscopy, functional diagnostics, etc.) [1, 2]. These methods provide a comprehensive idea of patient's actual health at the moment of measuring. Creation of evolution models is much more interesting since they are able to predict changes in public health depending on different environmental exposures, including life-threatening ones that can't be used in full-scale experiments. Mathematical modeling makes it possible to manage different exposures, consider their combinations, investigate and predict behavior of such a complicated system as the human body.

The authors have been developing a multi-level model [3] that considers the human body as a finite set of organs (systems) interacting with each other. Approaches to assessing individual and public health risks caused by exposure to heterogeneous environmental factors have been developed based on this multi-level model [4]. The macro-level concentrates on how functional disorders occur in the body due to its natural ageing and negative effects produced by environmental factors. The meso-level describes processes occurring in specific systems in the body in greater detail and the micro-level deals with processes developing in cells. A submodel of the respiratory system [5, 6] is included into the overall mathematical model describing evolution of functional disorders in the human body. This model is a meso-level one and can be considered a separate model due to its complexity.

[*]cinker@fcrisk.ru

The existing mathematical models of the respiratory system can be divided into structural and functional (statistical) ones. Statistical models are most frequently used in evidence-based medicine. They make it possible to establish cause-effect relations at the population level. In such models, the respiratory system is represented by ‘a black box’ within the ‘ambient air–black box–incidence’ or ‘ambient air–black box–blood’ systems. Such models identify reliable relationships between chemical levels in ambient air and health disorders [7, 8] but do not analyze processes occurring inside the system. Failure to get an insight into mechanisms and causes of health disorders makes it difficult to develop effective disease prevention.

Structural models are built based on laws and hypotheses about how a biological system is structured and how it operates. Mathematical models of the respiratory system can differ substantially depending on aims of a given study. Breathing mechanics employs models of various complexities in order to consider different mechanical processes. Starting from the middle of the last century and up to now, specific models have been widely used; they consider the lungs to be elastic membranes connected with the atmosphere by a tube with certain hydraulic resistance [9]. Such models make it possible to get the simplest relations between physical parameters that describe how the lungs operate but they do not consider spatial heterogeneity of respiratory processes in the human lungs.

The article [10] presents a short review of models that describe the human lungs. They differ in their complexity starting from those that consider the lungs a rigid container connected with the atmosphere and going to a model that describes how the volume and pressure change due to muscle efforts (a similar to a vessel with a plunger) and covers gas exchange with blood and blood perfusion. These models explain basic physiological processes occurring during breathing but they do not consider the actual geometry and length of the human airways.

The study [11] describes a two-chamber model of the lungs consisting of two spaces, an anatomically dead and alveolar one; blood perfusion is effected through the latter. The suggested model is applied to estimate a circulation volume per minute (cardiac output). The study contains mass balance equations for oxygen and carbon. The results yielded by the model are consistent with cardiac output measurements in six young healthy people obtained by the direct Fick method. The model, however, has a disadvantage, which is impossibility to trace changes in airflow parameters in different sections of the lungs.

The article [12] presents a one-dimensional model of airflow from the trachea to alveoli allowing for gas exchange (oxygen and carbon) with blood and blood perfusion. The authors assume that the airways have the correct dichotomy and that airflow is laminar. Existence of exactly 23 generations of airways has been explained based on this work: 23 generations of airways provide the most effective oxygen saturation and carbon removal with minimal resistance. Similar results are reported in the work [13].

Since methods and means of computational gas dynamics have been developing quite intensively, more and more attention is now paid to three-dimensional models describing airflow as a multi-component gas mixture moving inside channels with complex shapes [14–20]. In the work [14], the focus is on investigating airflow in the large airways under forced exhalation. The airways are modeled with three generations of bronchi, starting from the trachea, and are given in two variants (symmetric and asymmetric branching). Several works published by a team of authors from the Khristianovich Institute of Theoretical and Applied Mechanics of the Siberian Branch of the RAS [15–17] investigate airflow in the upper airways based on numeric modeling. Three-dimensional geometry of the nasal cavity is based on several tomograms made in parallel cross-sections. Airflow is described with the Navier–Stokes equations, and the ANSYS Fluent software package is applied to solve them. The authors have computed characteristics of the flow field in the nasal cavity under various respiratory exertions and visualized the results. It is noted that nasal cavities tend to have quite a variety of shapes and, consequently, airflow in them has very different structures.

The study [18] addresses how particles with different diameters move along the human airways. The airways are represented by seven generations of air-bearing channels with the oral cavity, throat, and larynx; their geometry is based on MRI images. The authors describe trajectories of particles with their diameter being 2.5, 5, 10, 20 and 30 micrometers. The work [21] reports the results obtained by numeric modeling of airflow in the completely lower airways, from the trachea to alveoli. Three-dimensional geometry of large airways is based on tomograms of the human lungs. Smaller airways are described with a one-dimensional model. The lung space from the large airways to the lung surface is homogeneously filled with small airways (considering evenly distributed lung acini). The suggested model is employed to investigate parameters of inhaled and exhaled airflow under normal breathing.

The existing three-dimensional models make it possible to trace how air moves from the atmosphere into the lungs and how chemicals are transferred with it at different moments of time. However, they describe only separate parts of the lungs, do not consider interactions between various organs in the human body, and do not give an opportunity to predict functional health disorders caused by harmful environmental exposures.

Given all the above stated, the aim of this study is to develop an evolution mathematical model of the respiratory system that considers environmental exposures. The developed model should provide an opportunity to describe how the respiratory system interacts with other systems in the human body and how damage accumulates in it due to natural ageing and harmful environmental exposures.

2. CONCEPTUAL STATEMENT

Respiration is a set of processes that provide oxygen introduction into blood and carbon removal from it (external respiration), use of oxygen by cells and tissues for oxidation of organic substances to release energy necessary for vital activity (cellular or tissue respiration). External respiration is provided by the respiratory system and consists of two basic processes, lung ventilation (gas exchange between the lungs and the atmosphere) and lung respiration (gas exchange between the lungs and blood). These two processes are considered in the present study.

The part of the respiratory system that provides external respiration contains the airways through which air is introduced into the lungs and the respiration section of the lungs where lung respiration occurs. The airways are divided into the upper and lower ones. The upper airways are the nasal cavity, nasopharynx, and oral pharynx. The lower airways are the larynx, trachea, extra- and intrapulmonary bronchi. Starting from the trachea, the lower airways have a tree-like structure. The trachea divides into two primary bronchi that go to the right and left lung. The primary bronchi continue to divide in the lungs and as the branching continues, the later generations of bronchi have smaller length and diameter. According to the Weibel morphometric model, the airways have 23 generations [22]. The branching finishes with the alveoli; gas exchange with blood occurs through alveoli walls which are simultaneously walls of the pulmonary capillaries.

The human lungs are inside the chest bounded by the ribs and the diaphragm. Inhalation and exhalation occur due to muscle effort. Respiration is regulated by the central nervous system through control of oxygen and carbon levels in arterial blood and cerebrospinal fluid. The chest volume, together with the lung volume, changes due to the respiratory muscles (primarily the diaphragm). The process creates difference in pressures between the lungs and the atmosphere, which results in gas flows into the lungs and out of them. Respiration is shown schematically in Figure 1. Several basic components participate in respiration: the airways, the respiratory section of the lungs, the musculoskeletal system, and the respiration regulation system. Functional disorders of any of these components can lead to respiratory diseases and their severe clinical forms (respiratory failure) that disrupt homeostasis.

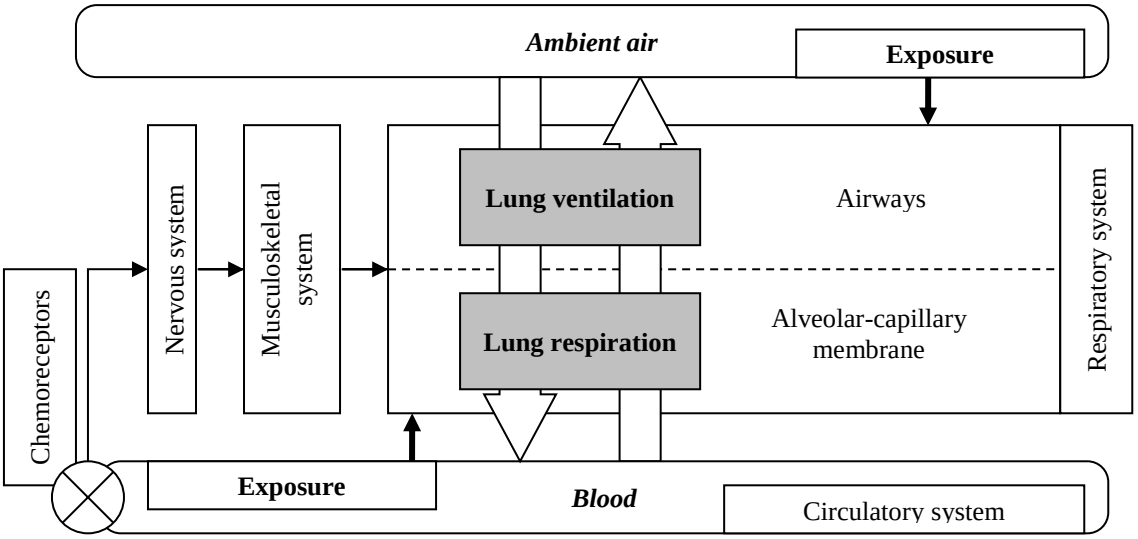

Fig. 1. The structure of the respiratory system.

Harmful chemicals that penetrate the human body from the environment produce toxic effects on its organs and systems, the respiratory system included. Environmental factors produce their toxic effects on the respiratory functions by two basic mechanisms: a single introduction of a high chemical dose or long-term exposure to low doses [23].

Structural disorders of the respiratory system become obvious through decrease functionality, which, in its turn, deteriorates gas exchange (by reducing diffusion capability of the alveolar-capillary membrane). In the multi-level mathematical model of the human body [3], reduced functional capabilities of the *j*-th organ (system) are described with damage $D_j(t)$, a parameter depending on time (age) *t*. Damage of organs can grow due to natural ageing and harmful environmental exposures; damage can also decrease due to treatment and organ self-recovery. Damage values vary between 0 and 1: if damage $D_j = 0$, a system operates normally (ideally), and if damage $D_j = 1$, it means a system is completely unable to perform its functions. Functionality of an organ (system) can be identified through damage since they are associated. Functionality $F_j(t)$ is an ability of an organ (system) to perform its functions. An association between damage of an organ and its functionality can be written, for example, as: $F_j(t) = (1 - D_j(t))^{n_j}$, $n_j \in R$, $n_j \geq 1$.

Generally, air is a gas suspension, that is, a multi-component mixture with solid particles in it. It is necessary to simulate air as a gas suspension in models when we have to describe respiration in dusty conditions, for example, in coalmines. If respiration occurs under dust-free conditions (that is, without any heterogeneous admixtures that are macroscopic against molecular scales), then air can be considered a multi-component gas mixture, which is homogeneous at a first approximation.

Modeling the breathing process, based on the representation of the respiratory organs in the form of a system of tubes (bronchi) ending in alveoli is difficult. It is due to the large branching of the bronchial system and the need to represent each alveoli in the form of a separate object with unique properties, resulting in a large number of ratios and parameters. We describe the respiratory system as consisting of the large airways (the first four generations starting from the trachea) entering the corresponding sections in the lungs. The lungs that are filled with smaller airways and alveoli, as well as air in them, can be depicted as a continuous deformable saturated porous medium placed in an internal chamber with a changing volume (moving walls).

These porous medium is saturated with gas. This is a two-phase continuous medium; its first phase is a deformable skeleton of the medium described with a model for deformable

solid body (to be more exact, nonlinear elastic model [24]); the second phase is a multi-component gas mixture that fills the porous space. All this space is assumed to be continuously filled with these two phases that are completely interpenetrating and interact with each other. The porous medium contains the alveolar-capillary membrane with its total area being equal to the total area of the alveoli through which gas exchange occurs by diffusion between air and blood. Oxygen comes to blood from air and carbon is released from it. Apart from oxygen and carbon, other chemicals occurring in ambient air participate in gas exchange. Respiration is regulated by the central nervous system through control of oxygen and carbon levels in blood.

In the reference configuration, lung tissue is in its natural relaxed state, oxygen and carbon levels in blood are within the reference ranges. When oxygen or carbon levels reach their critical value, the central nervous system gives a signal to relevant muscles. Under muscle effort, the internal chamber expands during inhalation, air near the entrance to the trachea, which is immovable at the initial moment, starts moving (from a high-pressure area to a lower pressure area). After entering the lungs, the gas mixture starts spreading in the porous medium. Gas exchange occurs through the alveolar-capillary membrane by diffusion of a chemical from an area where its concentration is high to an area where it is low. The alveolar-capillary membrane has different diffusion capabilities for different chemicals. After the lung, walls have been stretched to their maximum, inhalation finishes, and exhalation occurs due to the wall contraction. One human respiratory cycle (inhaling and exhaling) on average takes 4 seconds.

The mathematical model of the respiratory system (MMRS) is considered a set of three interrelated submodels:

1) The submodel describing how air moves in the large airways;
2) The submodel describing how air spreads in the deformable saturated porous medium in the lungs;
3) The submodel of gas exchange through a biological membrane.

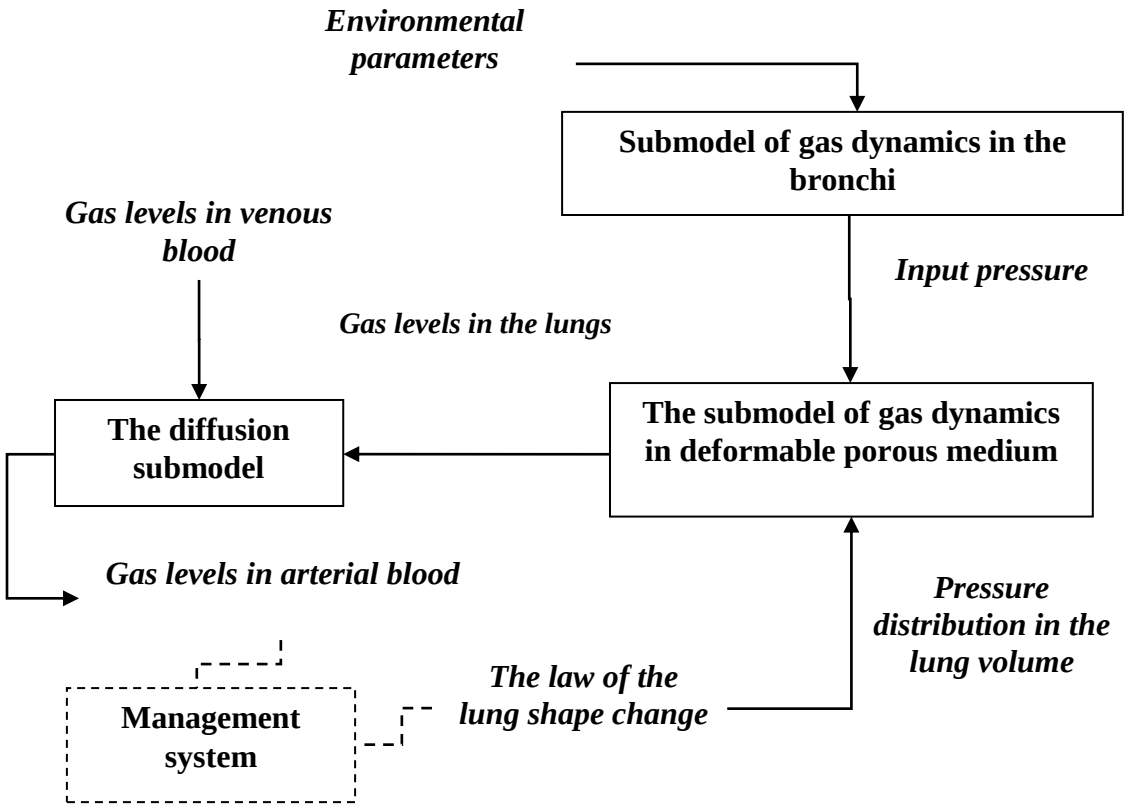

Fig. 2. The scheme showing interrelations between the submodels of the respiratory system.

Mathematical Biology and Bioinformatics. 2023. V. 18. № S. doi: 10.17537/2023.18.t38

This article contains the mathematical statement for the whole model of the respiratory system but main attention is paid to the first submodel that describes how air moves in the large airways.

Figure 2 provides the scheme showing how the submodels of the respiratory system interact with each other. At the model ‘input’, environmental parameters are specified. At the model ‘output’, we see chemical levels in blood and exhaled air. Arrows show interrelations between the submodels. Output data of one submodel are simultaneously input ones for another.

It is noteworthy that a gas dynamics problem is set in terms of Euler variables whereas deformable solid body requires Lagrange variables and setting in terms of the reference configuration.

In general, the mathematical model of the human respiratory system consisting of three submodels is essentially nonlinear. This necessitates using a systematic procedure when finding solution to the problem. Data are exchanged between the submodels at each time step. The iteration procedure describes the alternating sequence of the following stages: ‘change in the lung shape – change in pressure inside the lungs - change in pressure in the bronchi – air movement – gas exchange (changes in gas levels in blood) – change in …’.

Figure 3 shows the computed scheme of the human respiratory system that includes the large airways and the lung section filled with the porous medium. Pressure at the entry to the trachea equals the atmospheric pressure. Pressure at the exit from the bronchi is equal to pressure at the entry to the lungs (conjugation of two areas) and is identified at each computed step by using the iteration procedure.

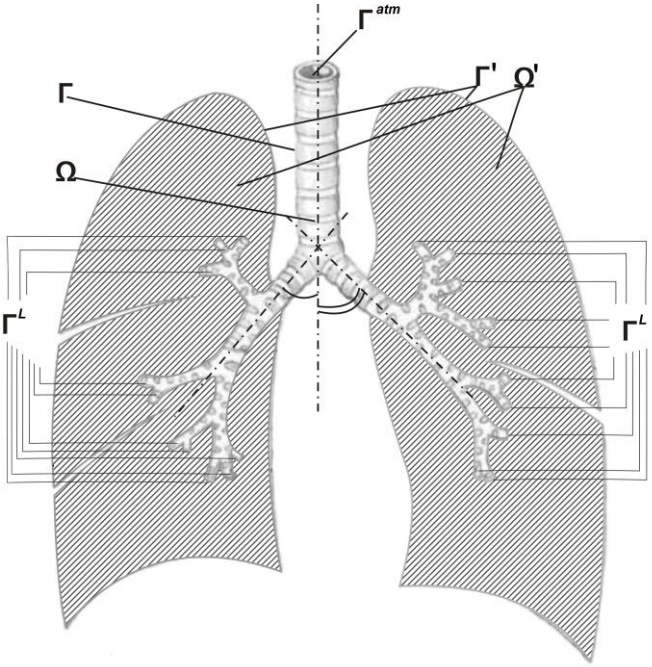

Fig. 3. The scheme of the human respiratory system.

3. MATHEMATICAL STATEMENT

The submodel of airflow in the large airways

Airflow of a multi-component gas mixture in the large airways is described with the system of Euler equations with added with the general gas equation:

$$\frac{\partial \rho_i}{\partial t} + \nabla \cdot (\rho_i v_i) = 0, \qquad \boldsymbol{r} \in \bar{\Omega},\ t \in [0;T), \tag{1}$$

$$\frac{\partial}{\partial t}(\rho_i \mathbf{v}_i) + \nabla \cdot (\rho_i \mathbf{v}_i \mathbf{v}_i) + \nabla p_i = 0, \qquad \mathbf{r} \in \Omega,\ t \in [0;T), \tag{2}$$

$$\frac{\partial \rho_i E}{\partial t} + \nabla \cdot (\rho_i E \mathbf{v}_i) + \nabla \cdot (p_i \mathbf{v}_i) = 0, \qquad \mathbf{r} \in \bar{\Omega},\ t \in [0;T), \tag{3}$$

$$p_i = \rho_i R\theta, \qquad \mathbf{r} \in \bar{\Omega},\ t \in [0;T). \tag{4}$$

Here ρ_i is the density of the *i*-th component in the gas mixture; $\mathbf{v}_i$ is the velocity of the *i*-th component in the mixture; E is the total specific energy of the mixture; p_i is pressure; R is the universal gas constant; θ is the mixture temperature; t is time, T is the upper boundary of the time variable; $\mathbf{r}$ is the radius-vector; Ω is the area interior; Γ is the area Ω boundary; and $\bar{\Omega} = \Omega \bigcup \Gamma$ is the closed area. It should be noted that all the tensor (vector) parameters are given in bold, both here and below in the text.

At the initial moment of time, pressure is homogeneous and the airflow velocity is equal to zero. Pressure is equal to the atmospheric pressure at the entry to the trachea. Pressure at the exit from the bronchi is equal to that at the entry to the lungs and is identified by the iteration procedure as per the pressure at the entry to the lungs identified by the solution to the problem for the porous medium form the previous iteration. The airway walls are specified as impermeable. In accordance with all the above stated, the entire initial and boundary conditions can be described by the following relationships.

The initial conditions:

$$\mathbf{v}_j(0,\ \boldsymbol{r}) = \mathbf{0}, \qquad \mathbf{r} \in \bar{\Omega},\ t = 0, \tag{5}$$

$$p_i = p_{\text{atm}}, \qquad \mathbf{r} \in \Gamma^{\text{atm}}. \tag{6}$$

The boundary conditions at a part of the boundary Γ are written as:

$$v_{in}\big|_{\Gamma} = 0, \qquad \mathbf{r} \in \Gamma,\ t \in [0;T), \tag{7}$$

where v_{in} is the normal component of the velocity vector for the *i*-th component in the mixture.

The submodel of air spreading in the deformable saturated porous medium of the lungs

Air spreading in the deformable saturated porous medium of the lungs is described with a system of equations. It includes the mass conservation equations for the gaseous and solid phases, the impulse conservation equation for the solid phase, the Darcy equation to describe relative movement of gas in the porous medium of the lungs, and physical and kinematic (Cauchy – Green stress tensor) relationships.

The mass conservation equations for the gaseous and solid phases are written as:

$$\frac{\partial \rho_i}{\partial t} + \hat{\nabla}(\rho_i \mathbf{v}_i) = 0, \qquad \mathbf{r} \in \bar{\Omega}',\ t \in [0;T), \tag{8}$$

$$\frac{\partial \rho_s}{\partial t} + \hat{\nabla}(\rho_s \mathbf{w}) = 0, \qquad \mathbf{r} \in \bar{\Omega}',\ t \in [0;T), \tag{9}$$

where $\hat{\nabla}$ is the Hamiltonian operator identified in the current (actual) configuration, ρ_s is the solid phase density in the porous medium, $\mathbf{w}$ is the velocity vector of the solid phase.

The impulse conservation equation is written as:

$$\frac{\partial \rho_s \mathbf{w}}{\partial t} = -\hat{\nabla}(\rho_s \mathbf{w}\mathbf{w}) + \rho_s \mathbf{g} - \hat{\nabla} \cdot \boldsymbol{\sigma}, \text{ where } \mathbf{w} = \frac{d\mathbf{u}}{dt}, \qquad \mathbf{r} \in \Omega',\ t \in [0;T), \tag{10}$$

where $\boldsymbol{\sigma}$ is the Cauchy stress tensor, $\mathbf{u}$ is the displacement vector, $\mathbf{g}$ is the density of volume forces (per a unit of mass).

The gaseous medium participates in two motions: transportation notion together with the deformable porous medium and relative motion due to permeation described by the Darcy law.

The Darcy equation that describes relative motion of a gas in the porous medium is written as:

$$\mathbf{v}_i = -\frac{k_i(\mathbf{C})}{\mu_i}\hat{\nabla}(p_i + \rho_i g z), \qquad \mathbf{r} \in \Omega',\ t \in [0;T) \tag{11}$$

where $\mathbf{v}_i$ is the filtration velocity vector of the *i*-th component in the mixture, $k_i(\mathbf{C})$ is the filtration coefficient, μ_i is dynamic viscosity, $\mathbf{C}$ is the Cauchy – Green stress tensor, z is the vertical coordinate, g is the free fall acceleration.

A hyperelastic constitutive law is applied as physical relationships:

$$\mathbf{K} = \frac{\partial A}{\partial \mathbf{C}}, \tag{12}$$

where $\mathbf{K}$ is the second Piola–Kirchhoff stress tensor.

A relation between the second Piola–Kirchhoff stress tensor and the Cauchy stress tensor is identified as per the following relationship:

$$\boldsymbol{\sigma} = (\hat{\rho}/\overset{o}{\rho})\overset{o}{\nabla}\mathbf{r}^T \cdot \mathbf{K} \cdot \overset{o}{\nabla}\mathbf{r}, \tag{13}$$

where $\overset{o}{\nabla}$ is the Hamiltonian operator identified in the reference configuration, $\hat{\rho}$ is the density in the current configuration, $\overset{o}{\rho}$ is the density in the initial configuration, $\mathbf{r}$ is the radius-vector of the solid phase particles.

The Murnaghan equation of state is used to identify potential energy A [24]:

$$A = \frac{1}{2}(\lambda + 2\nu)J_1(\mathbf{C})^2 - 2\nu J_2(\mathbf{C}) + \frac{1}{3}(l + 2m)J_1(\mathbf{C})^3 - 2mJ_1(\mathbf{C})J_2(\mathbf{C}) + nJ_3(\mathbf{C}), \tag{14}$$

where λ, ν are Lame constants; l, m, n are coefficients; $J_1(\mathbf{C})$, $J_2(\mathbf{C})$, $J_3(\mathbf{C})$ are the principal invariants of the stress tensor

The Cauchy–Green stress tensor is identified as per the displacement field and the following relationship:

$$\mathbf{C} = \frac{1}{2}(\overset{o}{\nabla}\mathbf{u} + (\overset{o}{\nabla}\mathbf{u}) + \overset{o}{\nabla}\mathbf{u}(\overset{o}{\nabla}\mathbf{u})^T), \quad \mathbf{r} \in \bar{\Omega}',\ t \in [0;T). \tag{15}$$

Pressure is identified for the gas phase within cross-sections of the point where the airways enter the lungs from the sub-problem of gas dynamics in the bronchi. Flows without separation and impermeability are specified at the lung walls:

$$v_{in}\big|_{\Gamma'} = v_n^{wall}, \qquad \mathbf{r} \in \Gamma',\ t \in [0;T), \tag{16}$$

where v_n^{wall} is the normal velocity component of the moving solid boundary.

In the reference configuration, lung tissues are relaxed naturally. The boundary kinematic-type conditions are used as boundary conditions for the elasticity problem:

$$\mathbf{u} = \hat{\mathbf{u}}_{\Gamma'}, \qquad \mathbf{r} \in \Gamma',\ t \in [0;T). \tag{17}$$

Diffusion from the alveolar-capillary barrier is described with an equation based on the Fick's First Law of Diffusion [25]. Diffusion capabilities of the lungs depend on the membrane functional state. The functionality of the alveolar-capillary membrane F takes a value within the range [0;1]. The chemical diffusion equation is written as:

$$\tilde{Q}_i = K_i F\left(\tilde{C}_{i1} - C_{i2}\right), \qquad \mathbf{r} \in \bar{\Omega}',\ t \in [0;T), \tag{18}$$

where $\tilde{Q}_i$ is the local flow of the *i*-th chemical from air into blood, $\tilde{C}_{i1}$, C_{i2} are the local levels of the *i*-th chemical in air inside the lungs and blood, K_i is the coefficient of the membrane permeability for the *i*-th chemical, *F* is the functionality of the alveolar-capillary membrane.

4. RESULTS

The complete mathematical model of the human respiratory system is rather complicated and includes a set of relationships that describe gas dynamics processes, porous medium deformation and diffusion; each process has certain peculiarities. This article reports the results of computing characteristics of airflow in the trachea and large bronchi since this part of the airways has complex asymmetric geometry and airflow inside it is rather complicated. This should be considered when creating models to describe the respiratory system. Further development of the model involves creating an algorithm and a subprogram for analyzing stressed-deformed condition and gas medium motion in the deformable saturated porous medium of the lungs filled with smaller airways.

Table 1. Diameter and length of some section in the lower human airways (1–4 generations) taken from literature sources and considered into the model

Source	Generation in the airways									
	1		2				3		4	
	Airways									
	Trachea		Left primary bronchus		Right primary bronchus		Lobar bronchi		Segmental bronchi	
	*d**	*l**	*d*	*l*	*d*	*l*	*d*	*l*	*d*	*l*
Weibel [22]	18	120	12.2	47.6	12.2	47.6	8.3	19	5.6	27.6
Sinel'nikov et al[26]	15–27	90–150		40–50		30				
Sapin [27]	15–18	90–110		40–50		30				
Kukes et al.[28]	15–25	м – 140 ж – 120	8–16	40–50	12–22	30				
Zolotko [29]		80–150	9–20	45–60	14–23	20–30				
MMRS	**15**	**100**	**12**	**50**	**14**	**30**	**8.3**	**21**	**5.6**	**27.6**

**d* is diameter (mm), *l* is length (mm).

Three-dimensional geometry of the first four generations in the lower airways is based on available literature data and expert consultations provided by healthcare practitioners. According to literature data, the airways tend to be quite different from person to person. Table 1 provides some examples (diameter and length) of bronchial tree sections taken from different literature sources.

Such a wide range of geometric properties can occur due to individual anatomic features of examined people. The primary bronchi angles also vary depending on build. Table 2 provides some values of the primary bronchi angles (from the sagittal plane (see Figure 3)) taken from different sources.

Medical atlases provide comprehensive data about sizes and angles of the trachea and primary bronchi but any data on smaller airways are not available [26–30].

Table 2. The primary bronchi angles taken from literature sources and considered in the model

Source	The primary bronchi angle form the sagittal plane

	Left primary bronchus	**Right primary bronchus**
Kukes et al.[28]	50–70º	15–40º
Zolotko [29]	18–54º	12–40º
Morgan et al. [30]	45º	25º
MMRS	**50º**	**30º**

The study by E.R. Weibel [22] (Table 1) contains the most comprehensive description of qualitative properties (diameter and length) for all the airway generations. The model suggested by Weibel is based on research data obtained by dissection of healthy lungs and bronchograms of healthy people; however, it assumes that the airways have the correct dichotomy and this is not consistent with the actual human bronchial tree. In addition, Weibel does not provide any data on branching angles of the airways (Table 2).

Therefore, our created geometry of the human respiratory system was based on the Weibel model (since it provides qualitative properties of the lobar and segmental bronchi); it was adjusted based on data taken from medical reference books and on consultations given by healthcare practitioners. The major addition involved adjusting the primary bronchi sizes and angles; this allowed considering the incorrect dichotomy of the bronchial tree (the right primary bronchus angle is smaller than the left primary bronchus angle; the right primary bronchus is shorter than the left primary bronchus). Table 1 provides diameters and lengths of some sections in the lower airways (1–4 generations). The primary bronchi angles were taken from medical reference books (Table 2).

The right lung consists of three lobes; the left lung, two. Each lobe consists of segments. Each lung has 10 segments. The lobar bronchi are a part of lung lobes and the segmental bronchi are located in relevant segments. One entry has a common boundary with the atmosphere in the respiratory system model, namely, the trachea. There are 20 entries to the lungs in it, which correspond to the segmental bronchi (3 in the upper lobe of the right lung; 2 in the middle lobe; 5 in the lower lobe; 5 in the upper and lower lobe of the left lung). Figure 4 shows the created three-dimensional geometry of the airways in axonometry (frontal view).

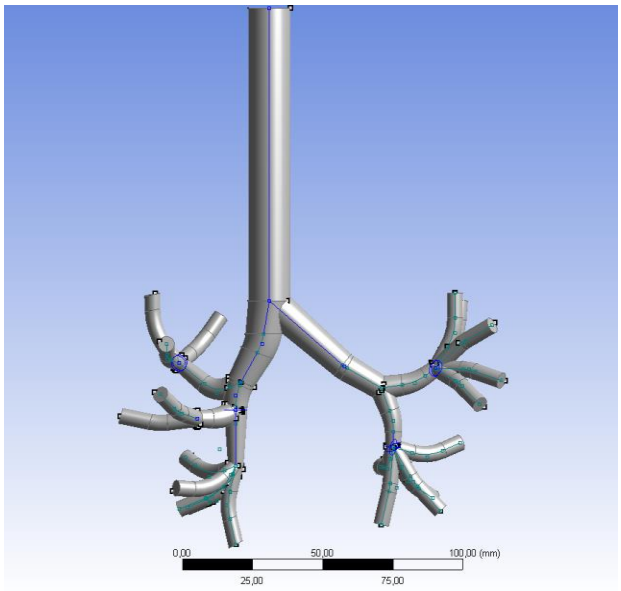

Fig. 4. Three-dimensional geometry of the airways in axonometry (frontal view).

Airflows in the large airways are computed with the ANSYS Fluent software package. We have computed two scenarios, a model of relaxed breathing (inhalation and exhalation) and forced inhalation in healthy people.

Pressure at the entry and exit are specified as initial conditions. In each scenario, pressure at the entry to the trachea is set as equal to the atmospheric air pressure (760 mm Hg or 101,325 Pa). Pressure at the exit from the bronchi is set as below the atmospheric air pressure during inhalation and above it during exhalation. In healthy people, intra-alveolar pressure changes by 1 cm w.c. (95 Pa) under relaxed breathing [25]. Therefore, pressure at the exit from the bronchi is equal to 101,226 Pa for inhalation and 101,423 for exhalation. Under forced inhalation, pressure at the exit from the bronchi is set 3 mm HG below the atmospheric air pressure (100,925 Pa). Therefore, we obtain airflow parameters under two scenarios. The velocity vector fields under relaxed breathing are shown in Figures 5 (inhalation) and 6 (exhalation).

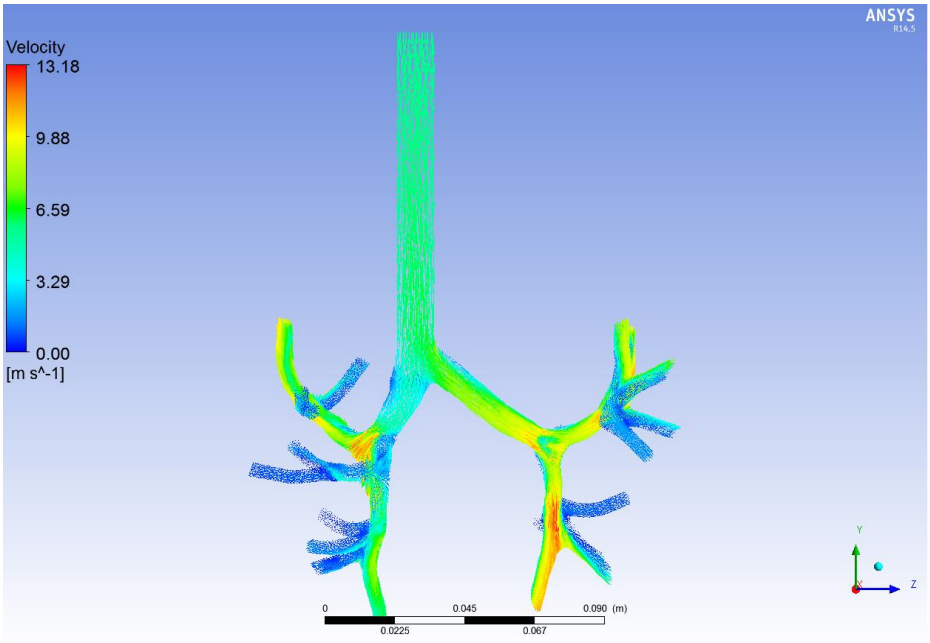

Fig. 5. The velocity vector field under relaxed inhalation in axonometry (frontal view).

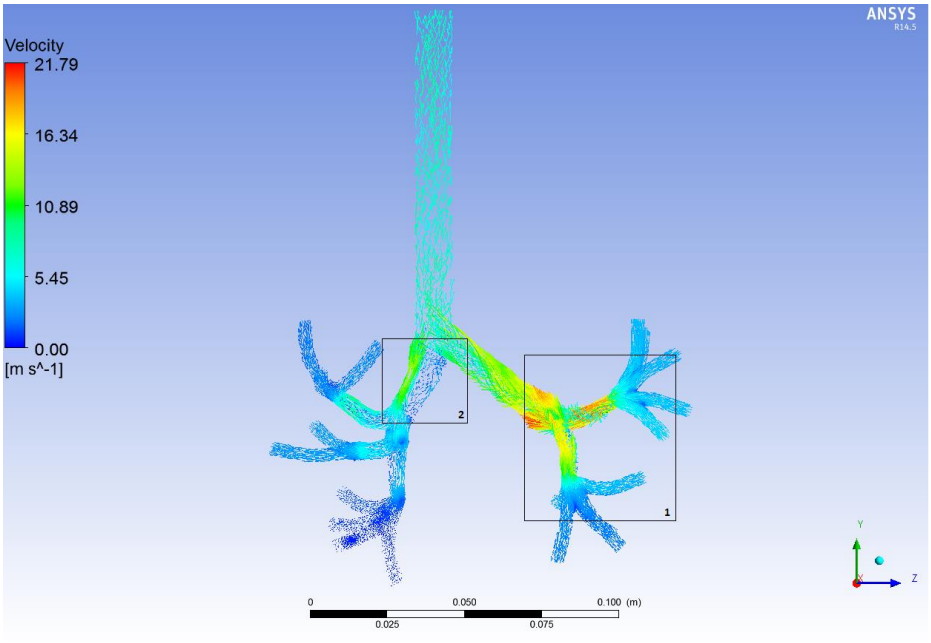

Fig. 6. The velocity vector field under relaxed exhalation in axonometry (frontal view).

Under relaxed inhalation, the airflow velocity in the trachea equals approximately 6.5 m/s; the maximum velocity occurs in the left lobar bronchus where it amounts to 18.18 m/s. Overall, as airway diameters decrease, airflow velocities also go down. This is due to the total

area of cross-sections at the entry to the lungs being bigger than the area of the trachea cross-section. The lowest velocities are detected in the segmental bronchi. Airflow velocity is higher in the left primary bronchus than in the right one due to the diameter of the former being smaller than that of the latter. Airflow velocities tend to increase at points where the airways get narrower or where they branch out.

Under relaxed exhalation, airflow velocity in the trachea is approximately 9 m/s. The highest velocities occur at the point where the left primary bronchus branches out into the lobar bronchi. Figure 7 shows an enlarged image of the velocity field in the bifurcation area of the left primary bronchus, which is highlighted in Figure 6 (Fragment 1).

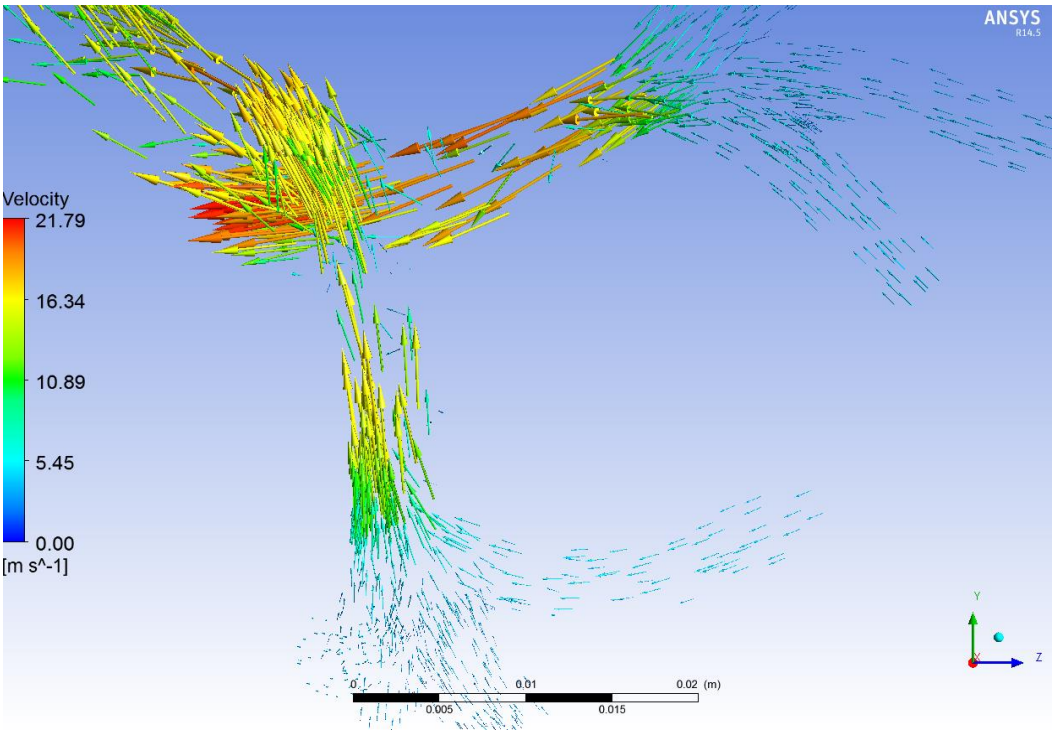

Fig. 7. The velocity vector field in axonometry (frontal view) (enlarged fragment 1, which was highlighted in Figure 6).

The smallest airflow velocity is in the segmental bronchi. As the airways get larger, airflow velocities also grow. This is due to the total area of the airway cross-sections at the entry to the lungs being bigger than the area of the trachea cross-section. The maximum velocity at the branching point reaches 21.79 m/s.

Vorticity is detected at the points where the airways branch out. Figure 8 shows an enlarged image of the velocity field in the area where the trachea divides into the primary bronchi (it is highlighted in Figure 6, fragment 2). Under relaxed exhalation, an airflow vortex occurs in the right primary bronchus.

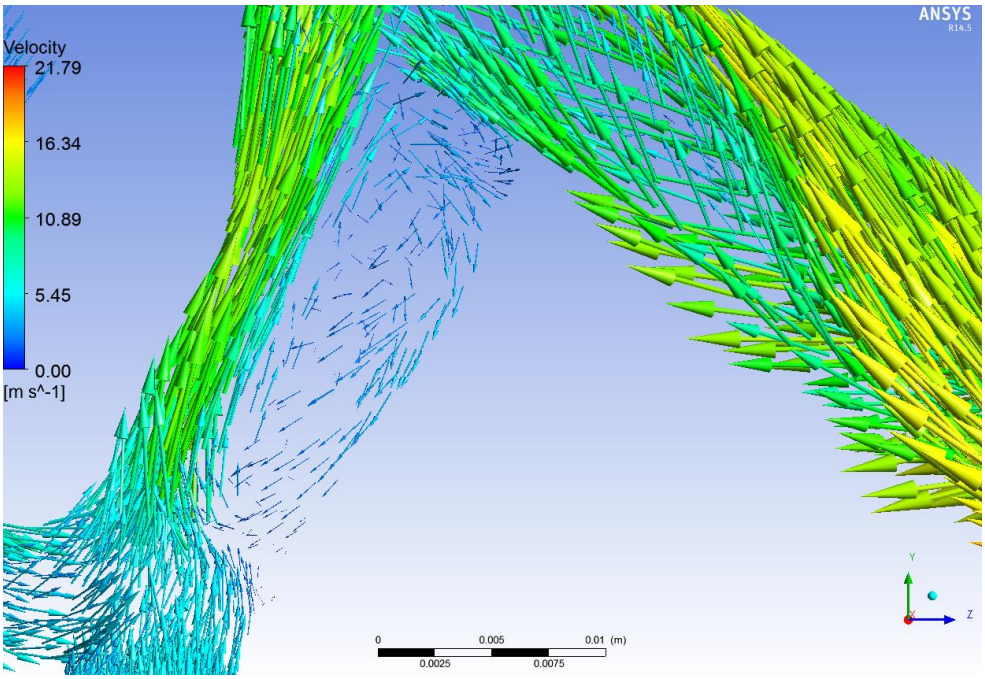

Fig. 8. The velocity vector field in axonometry (frontal view) (enlarged fragment 2, which was highlighted in Figure 6).

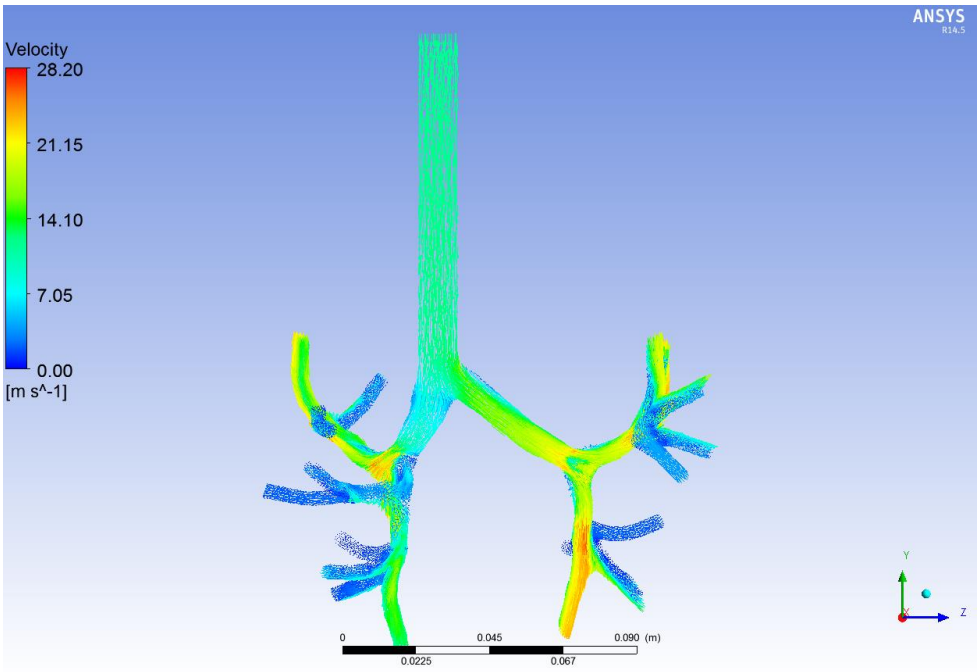

Fig. 9. The velocity vector field under forced inhalation in axonometry (frontal view).

Figure 9 shows the velocity vector field under forced inhalation.

Under the second scenario (forced inhalation), airflow remains the same in its nature as under relaxed inhalation.

As opposed to relaxed inhalation, airflow velocities increase in each section of the airways. The airflow velocity in the trachea is approximately 13 m/s. The highest velocities occur in the left primary bronchus. The maximum airflow velocity equals 28.2 m/s in this scenario.

It is noteworthy that pressure at the exit from the bronchi (at the boundary Γ^L) is the same in each scenario, which is justified since pressure in the lungs is also the same. When the

lungs are modeled as a deformable saturated porous medium, pressure will be different in their different sections.

Further development of the model will involve finding combined solutions to problems of gas dynamics in the large airways and air spread in the deformable porous medium of the lungs. The results concerning gas flows in the lungs will be reported in our future articles.

Therefore, we have considered the mathematical model of the human respiratory system. It is a meso-level submodel of the macro-level model describing the whole human body. The respiratory system model consists of three interrelated submodels that describe breathing as a set of synchronized gas dynamics processes in the bronchi, gas mixture notion in a deformable saturated porous medium, and diffusion. At this stage, we have applied the ANSYS Fluent software package to compute airflow under relaxed breathing and forced inhalation in the first four generations of the airways starting from the trachea. Further development of the model involves finding combined solutions to problems concerning deformation of the lungs and gas dynamics in the human airways.

REFERENCES

1. Shkliar B.S. *Diagnostika vnutrennikh boleznei* (Diagnostics of Internal Diseases). Kiev: Vysshaya Shkola, 1972. 516 p. (in Russ.).
2. Grebenev A.L. *Propedevtika vnutrennikh boleznei* (Propaedeutics of Internal Diseases). M.: Meditsina, 2001. 592 p. (in Russ.).
3. Trusov P.V., Zaitseva N.V., Kiryanov D.A., Kamaltdinov M.R., Cinker M.Ju., Chigvintsev V.M., Lanin D.V. A Mathematical model for evolution of human functional disorders influenced by environment factors. *Mathematical Biology & Bioinformatics*. 2012. V. 7. No. 2. P. 589–610 (in Russ.). doi: 10.17537/2012.7.589
4. Zaitseva N.V., Trusov P.V., Shur P.Z., Kiryanov D.A., Chigvintsev V.M., Tsinker M.Yu. Methodical approaches to health risk assessment of heterogeneous environmental factors based on evolutionary models. *Health Risk Analysis*. 2013. V. No. 1. P. 15–23 (in Russ.).
5. Tsinker M.Yu. In: *Biomechanics – 2014*: Proceedings of the XI All-Russia Conference with International Participation and Workshop-School for Young Scientists (Perm', 1-4 December 2014) Perm': Perm' National Research Polytechnic University Press, 2014. V. 1. P. 290–292 (in Russ.).
6. Tsinker M.Yu. A mathematical model of the human respiratory system. In: *Biomechanics – 2014*: Proceedings of the XI All-Russia Conference with International Participation and Workshop-School for Young Scientists (Perm', 1-4 December 2014). Perm': Perm' National Research Polytechnic University Press, 2014. P. 255–258 (in Russ.).
7. Onishchenko G.G., Zaitseva N.V., Zemlyanova M.A. *Hygienic indication of health effects at environment exposure of chemical factors*. Ed. Onishchenko G.G. Perm': Knyzny Format, 2011. 532 p.
8. Zaitseva N.V., Ustinova O.Yu., Aminova A.I. *Hygienic aspects of health disorders in children exposed to chemical environmental*. Ed. Zaitseva N.V. Perm': Knyzny Format, 2011. 489 p.
9. Lyubimov G.A. Models of Human Lungs and Investigation of the Respiration Mechanics on the Basis of these Models. *Proceedings of the Steklov Institute of Mathematics*. 1998. V. 223. P. 196–205.
10. Ben-Tal A. Simplified models for gas exchange in the human lungs. *Journal of Theoretical Biology*. 2006. V. 238. P. 474–495. doi: 10.1016/j.jtbi.2005.06.005

11. Benallal H., Beck K.C., Johnson B.D., Busso T. Evaluation of cardiac output from a tidally ventilated homogeneous lung model. *Eur. J. Appl. Physiol*. 2005. V. 95. P. 153–162. doi: 10.1007/s00421-005-1376-6
12. Kuwahara F., Sano Y., Liu J., Nakayama A. A Porous Media Approach for Bifurcating Flow and Mass Transfer in a Human Lung. *J. Heat Transfer*. 2009. V. 131. No. 10. doi: 10.1115/1.3180699
13. Reis A.H., Miguel A.F., Aydin M. Constructal theory of flow architecture of the lungs. *Journal of Medical Physics*. 2004. V. 31. P. 1135–1140. doi: 10.1118/1.1705443
14. Kirillova I.V., Gramakova A.A., Belova Iu.A., Chelnokova N.O. In: *Metody komp'iuternoi diagnostiki v biologii i meditsine - 2009* (Computer Diagnostics Methods in Biology and Medicine - 2009): Proceeding of Annual All-Russia Scientific Workshop-School. Ed. Usanov D.A. Saratov: National Research Saratov State University Press, 2009 (in Russ.).
15. Fomin V.M., Vetlutsky V.N., Ganimedov V.L., Muchnaya M.I., Shepelenko V.N., Melnikov M.N., Savina A.A. Air flow in the human nasal cavity. *Journal of Applied Mechanics and Technical Physics*. 2010. V. 51. No. 2. P. 233–240. doi: 10.1007/s10808-010-0033-y
16. Fomin V.M., Ganimedov V.L., Mel'nikov M.N., Muchnaya M.I., Sadovskii A.S., Shepelenko V.I. Numerical modeling of the air flow in the human nasal cavity with simulation of application of the clinical method of active anterior rhinomanometry. *Journal of Applied Mechanics and Technical Physics*. 2012. V. 53. No. 1. P. 49–55. doi: 10.1134/S0021894412010075
17. Ganimedov V.L., Muchnaya M.I., Sadovskii A.S. Air flow in the human nasal cavity. Results of mathematical modelling. *Russian Journal of Biomechanics*. 2015. V. 19. No. 1. P. 31–44.
18. Lambert A.R. *Regional deposition of particles in an image-based airway model: CFD simulation and left-right lung ventilation asymmetry*: MS (Master of sciences) thesis. Iowa: University of Iowa, 2010. 68 p.
19. Wall W.A., Rabczuk T. Fluid structure interaction in lower airways of CT-based lung geometries. *Int. J. Num. Methods in fluids*. 2008. V. 57. P. 653–675.
20. Kleinstreuer. C., Zhanga Z., Lia Z., Roberts W.L., Rojasc C. A new methodology for targeting drug-aerosols in the human respiratory system. *International Journal of Heat and Mass Transfer*. 2008. V. 51. P. 5578–5589. doi: 10.1016/j.ijheatmasstransfer.2008.04.052
21. Choi J. *Multiscale numerical analysis of airflow in CT-based subject specific breathing human lungs*: PhD Dissertation. Iowa: University of Iowa, 2011. 259 p.
22. Weibel E.R. *Morfometriia legkikh cheloveka*. Moscow, 1970. 176 p. (Translation of: Weibel E.R. Morphometry of the Human Lung. Springer Verlag, Berlin-Göttingen-Heidelberg; 1963).
23. *Toxikologicheskaya khimiya. Metabolizm i analiz toksikantov*. (Toxicological Chemistry: Toxicant Metabolism and Analysis): Student's manual. Ed. Kaletina N.I. Moscow: GEOTAR-Media, 2008. 1016 p. (in Russ.).
24. Lurie A.I. *Theory of Elasticity*. Springer, 2005. 1050 p. doi: 10.1007/978-3-540-26455-2
25. *Fiziologiia dykhaniia. Osnovy*. Moscow: Mir, 1988. 196 p. (Translation of: West J.B. Respiratory Physiology - The Essentials. Lippincott Williams and Wilkins, USA; 1985).
26. Sinel'nikov R.D., Sinel'nikov Ia.R. *Atlas anatomii cheloveka* (Atlas of Human Anatomy). Moscow: Mir Publisher, 1996. 264 p. (in Russ.).

27. Borzyak E.I., Volkova L.I., Dobrovol'skaya E.A., Revazov V.S. *Human Anatomy*. Ed. Sapin M.R. Moscow: Medicine, 1993. V. 1. 544 p. (in Russ.).

28. Kukes V.G., Marinin V.F. *Clinical Diagnostic Methods (inspection, palpation, percussion, auscultation)*: Student's Manual. Moscow: GEOTAR-Media, 2006. 720 p. (in Russ.).

29. Zolotko Yu.L. *Topographic Atlas of Human Anatomy*. Moscow: Medicine, 1967. 272 p. (in Russ.).

30. Morgan G.E., Michael M.S. *Klinicheskaia anesteziologiia*. M.-SPb.: BINOM-Nevskii Dialekt, 2001. 396 p. (Translation of: Morgan G.E., Michael M.S. Clinical Anesthesiology. v. 2. Appleton & Lange A Simon & Schuster Company;1996. 747 p.).

Received 19.05.2023.
Published 12.08.2023.